Electronic Supplementary Information

Isothermal amplification of specific DNA molecules inside giant unilamellar vesicles

Yusuke Sato,*[a†] Ken Komiya,[b] Ibuki Kawamata,[a] Satoshi Murata,[a] and Shin-ichiro M. Nomura*[a]

Materials

The signal, converter, amplifier, and beacon DNAs were purchased from Gene Design (Ibaraki, Japan). Output DNA was purchased from Eurofins Genomics (Louisville, KY, USA). Caged-signal DNA was purchased from Tsukuba Oligo Service (Ushiku, Japan). Sequences of the DNAs used are shown in Table S1. The 3′ ends of the converter and amplifier DNA were modified by three inverted thymines to avoid undesired polymerisation. The 5′ and 3′ ends of the beacon DNA were labelled with a fluorescent molecule, Alexa 488, and a quencher molecule, DABCYL, respectively. The DNAs were dissolved in ultrapure water, and the stock solution was stored at −20°C. Deoxyadenosine triphosphate (dATP), deoxyguanosine triphosphate (dGTP), deoxycytidine triphosphate (dCTP), and deoxythymidine triphosphate (dTTP) were purchased form GeneACT (Kurume, Japan). Klenow fragment (3′→5′ exo–), Nb.BbVCI and NEBuffer2, consisting of 50 mM NaCl, 10 mM Tris-HCl (pH 7.9), 10 mM $MgCl_2$, and 1 mM DTT were purchased from New England Biolabs (Ipswich, MA, USA). Klenow fragment (3′→5′ exo–) is a mutant of DNA polymerase I, in which the 5′→3′ and 3′→5′ exonuclease activities are deactivated. Nb.BbVCI is a nicking enzyme that cuts one strand of double-stranded DNA at its recognition site. The enzymes were aliquoted and immediately stored at −20°C upon delivery.

1,2-Dioleoyl-sn-glycero-3-phosphocholine (DOPC) was purchased from NOF Corporation (Tokyo, Japan). Rhodamine B 1,2-dihexadecanoyl-sn-glycero-3-phosphoethanolamine (rhodamine-DHPE) was purchased from Thermo Fisher Scientific (Waltham, MA, USA). Cholesterol, glucose, trehalose, and bovine serum albumin (BSA) were purchased from Wako Pure Chemical Industries (Osaka, Japan). Stock solutions and mixtures of lipids and cholesterol were dissolved in chloroform and stored at –20°C. BSA was dissolved in ultrapure water at 10% (w/v) as follows: BSA powder was slowly

added to water in the tubes to avoid bubble formation, and the solution was left at 4°C overnight.

Table S1. DNA sequences used in the amplification circuit

Name and length	Sequence (5'-3')
Converter (47 nt)	AGCCCTGTACAATGCCCTCAGCCTGTTCCTGCTGAACTGAGCCA-idT-idT-idT
Amplifier (38 nt)	AGCCCTGTACAATGCCCTCAGCAGCCCTGT^{L}ACAAT-idT-idT-idT
LNA-free Amplifier	AGCCCTGTACAATGCCCTCAGCAGCCCTGTACAAT-idT-idT-idT
Beacon (19 nt)	[Alexa488]-AGCCCTGTACAATGCGGCT-[DABCYL]
Signal (22 nt)	TGGCTCAGTTCAGCAGGAACAG
Caged-Signal (60 nt)	TGGCTCAGTTCAGCAGGAACAG-X-TTTTCTG-X-TTCCTGC-X-TGAACTG-X-AGCCA
Output (20 nt)	TGAGGGCATTGTACAGGGCT

-idT- and -X- indicate inverted thymine and photocleavable sites, respectively.

^{L} in the amplifier sequence indicates the locked nucleic acid of the 6th thymine from the 3' end.

Methods

Amplification in test tubes

Changes in green fluorescence intensity were measured using a real-time PCR detection system (Bio-Rad, Hercules, CA, USA). The concentrations of converter, amplifier, and beacon DNAs were set to 20 nM, 50 nM, and 500 nM, respectively. The reaction mixture was prepared on ice in white 0.2-ml 8-Tube Strips (Bio-Rad, Hercules, CA, USA) to a final volume of 10 µL. Glucose and trehalose, which were not required for amplification, but were contained in the GUVs, were added to the mixture. After mixing all of the components on ice, the tubes were centrifuged and incubated at 37°C. Temperature-dependent behaviour of amplification was investigated using a real-time detection system with temperature gradient function at 32–46°C. Composition of the solution is

shown in Table S2.

Table S2. Final concentrations of components of the amplification mechanism in solution.

Component	Final concentration
Signal	0, 0.1, 1, or 10 nM
Converter	20 nM
Amplifier	50 nM
Beacon	500 nM
dNTP	400 μM
Klenow fragment (3′→5′ exo–)	0.1 U/μL
Nb.BbvCI	0.1 U/μL
Glucose	150 mM
Trehalose	150 mM
NEBuffer2	×1

Preparation of GUVs

GUVs were prepared using the emulsion transfer method.[1] The vesicle membrane was composed of DOPC:cholesterol at a molar ratio of 9:1. Sixty microliters of a 50 mM lipid mixture, containing 0.05 mol% RH-DHPE dissolved in chloroform, was poured in a glass tube, the solvent was evaporated under argon gas flow to obtain a lipid dry film, and further dried under a vacuum for at least over 2 h. After vacuum drying, 300 μL of liquid paraffin was added to obtain a final lipid concentration of 10 mM. Subsequently, the lipids in oil were sonicated at 50°C for at least 120 min. The osmolality of the inner and outer solutions of GUVs was measured using a vapour pressure osmometer (VAPRO Osmometer 5520; Wescor, Logan, UT, USA). Osmolality of the inner solution, containing the amplification components (DNAs, dNTP, and enzymes), glucose, and trehalose, was approximately 510 mmol/kg. Thus, osmolarity of the outer solution was adjusted to approximately 510 mmol/kg by adding glucose into NEBuffer2.

Twenty microliters of inner solution was added to 300 μL of the lipid mixture in

a glass tube, and the mixture was then vortexed for 15 s to obtain emulsions. The emulsion was poured onto the outer solution in a 1.5-mL test tube and centrifuged at 7,000 × *g* at 4°C for 15 min. After centrifugation, precipitated GUVs in the test tube were collected, and the solution containing GUVs was placed on ice until the observation period.

Amplification in GUVs

Observation glass slides were coated with 10% BSA. The BSA solution was placed on the glass and incubated at 25°C for 30 min, and then the glass was washed with distilled water. A 0.5-mm-thick silicone rubber sheet with a punch hole (5 mm in diameter) was placed on the BSA-coated glass. The sample solution was poured in the hole, and a coverslip was placed onto the silicone rubber. Amplification in GUVs was observed using a confocal laser-scanning microscope (FV-1000; Olympus, Tokyo, Japan) with a 20× objective lens (UPlanSApo; Olympus) and a stage incubator (MI-IBC; Olympus). Temperature of the sample region was set at 37°C, as determined by non-contact temperature measurement (830-T1; Testo, Lenzkirch, Germany). Note that the focus of the microscope was adjusted immediately after the sample was set on the stage heater, and thus the sample solution was incubated at 37°C for a few minutes before the observation.

Analysis of DNA amplification in bulk and GUVs

The fluorescence intensity curve obtained from the experiments was analysed by curve fitting.[2] Log-logistic curves were fitted to the data. Curve fitting was based on a five-parameter sigmoidal curve described by the following equation:

$$Intensity\ (t) = c + \frac{d - c}{(1 + exp(- b(\log(t) - \log(e))^f} \qquad (1)$$

where *b, c, d, e,* and *t* correspond to the slope, ground asymptote, maximum asymptote, inflection point, and time, respectively. The parameter f is an additional asymmetry parameter that provides an accurate fitting curve. The fitting parameters (*b, c, d, e*, and *f*) were estimated by a least-squares method using "solver" of Microsoft EXCEL, in which the parameters that minimise the residual sum-of-squares was sought.

Amplification in test tubes with large unilamellar vesicles (LUVs)

To investigate the effect of lipid membranes on amplification behaviour, changes in fluorescence intensity were monitored in test tubes containing LUVs composed of DOPC:cholesterol at a 9:1 ratio. LUVs were prepared using a mini-extruder kit with a polycarbonate membrane filter (diameter: 0.1 μm; Avanti Polar Lipids, Alabaster, AL, USA). A lipidic dry film was hydrated using ultrapure water, and the extrusion process was repeated 23 times. The LUV solution was added to the test tubes at final concentrations of 0.016 mM, 0.16 mM, and 1.6 mM, which correspond to approximately 1/10, 1, and 10 times the lipid concentration inside GUVs. The concentration was determined from the average radius of GUVs (11.0 ± 2.8 μm), analysed in this study, and the surface area of a single lipid molecule (0.65 nm^2).[3]

Estimation of the number of entrapped DNAs in GUVs based on Poisson distribution

The number of DNAs trapped inside GUVs was estimated based on Poisson distribution.[4] Poisson distribution is represented by the following equation:

$$p(N) = (\lambda^N/N!) \cdot exp(—\lambda)$$

where $\lambda = cVN_A$, N is the number of molecules trapped inside GUVs of volume V, N_A is Avogadro number, and c is molar concentration in bulk solution. We estimated the number fluctuation for 0.1 nM signal DNA, 20 nM converter DNA, and 50 nM amplifier DNA across the average size range of GUVs (8–14 μm in radius) measured in experiments.

DNA amplification in GUVs initiated by photo-stimulation

To demonstrate the initiation of amplification in GUVs by external stimulation, caged-signal DNA was used. The photo-cleavable site can be cut by irradiating light of wavelength around 300–350 nm.[5,6] To ensure that the signal sequence was covered before UV irradiation, the caged-signal was annealed at a concentration of 1 μM in NEBuffer2 for 90 min across a temperature range of 95°C to 5°C at a rate of –1°C/min using a thermal cycler.

To cut the photo-cleavable site, the annealed caged-signal was irradiated with 340-nm UV light using a 300 W Xenon light source (MAX303; Asahi Spectra, Tokyo, Japan). For investigating the time required for efficient photo-cleavage, the sample was irradiated with UV light for 0, 1, 2, 3, 4, or 5 min, and subjected to gel electrophoresis on 12% acrylamide gels at 100 V for 80 min at room temperature with light shielding.

Gels were stained with SYBR Gold for 15 min and imaged using a ChemiDoc gel imager (BioRad).

To confirm the initiation of amplification in GUVs by photo-stimulation, the annealed caged-signal was encapsulated into GUVs with the amplification reaction solution at 10 nM. Before UV irradiation, the prepared GUV sample was set on the stage incubator and visualised using the microscope for 30 min at 37°C to ensure that the amplification did not occur without photo-stimulation. The sample on the stage incubator was then irradiated with UV light, using the Xenon light source, for 5 min, and the same region (visualised before the irradiation) was observed once again.

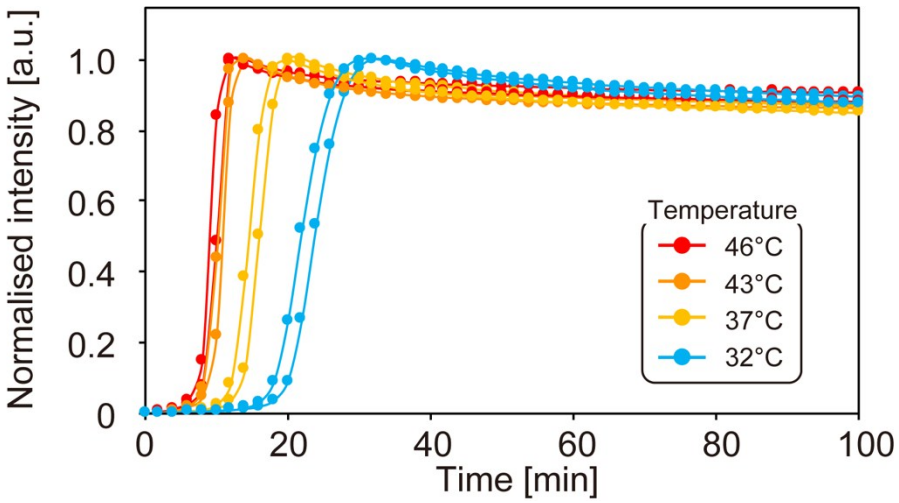

Fig. S1 Amplification reaction at different temperatures under 1 nM signal concentration. Increase of fluorescence intensity was detected at all temperatures (from 32°C to 46°C), thereby suggesting that the amplification circuit can function over a wide temperature-range. In addition, the rate at which fluorescence intensity reached a plateau was slightly faster with the rise of temperature. In this study, we focused on achieving isothermal amplification at 37°C, since this is the optimal temperature for most biochemical reactions. Therefore, we adopted 37°C for all our experiments.

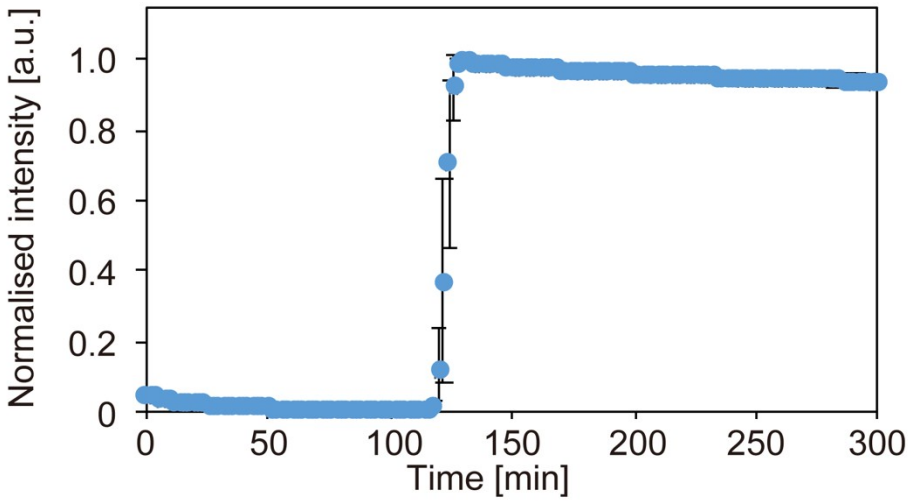

Fig. S2 Amplification reaction without signal DNAs, using the amplifier without LNA in test tubes. Despite the absence of signal DNAs, fluorescence intensity was found to increase, thereby suggesting the occurrence of non-specific amplification (leak amplification) when LNA was not included in the amplification circuit. Details of the

strategy for suppression of leak amplification was described by Komiya et al.[7]

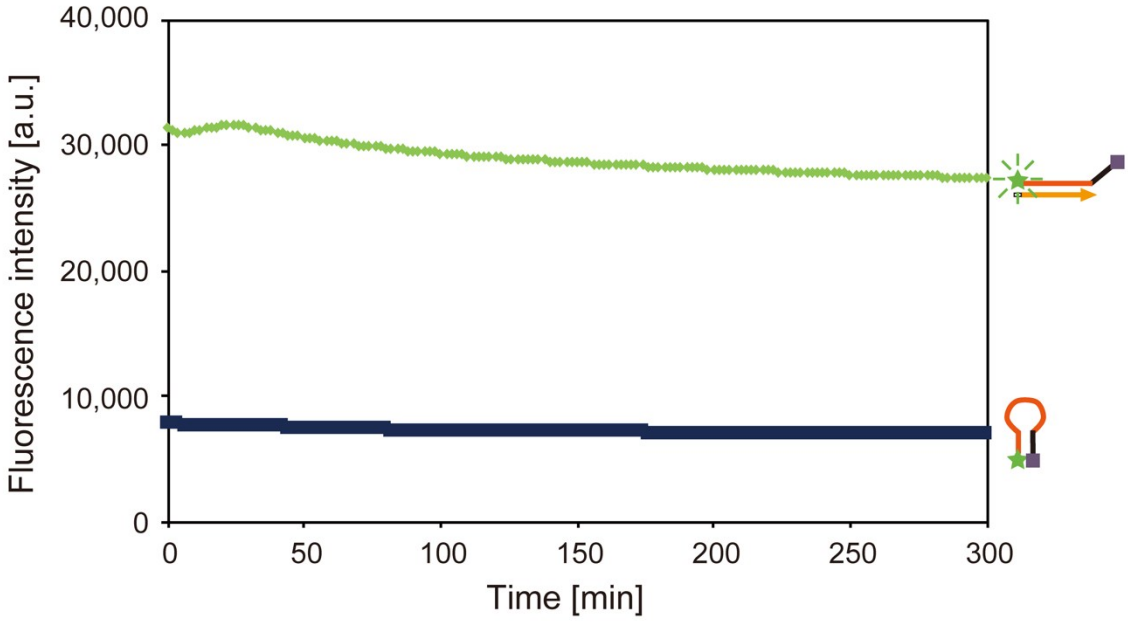

Fig. S3 Time series of fluorescence intensity for the opened-beacon (green) (with output DNA) and the closed-beacon (navy) (without output DNA).

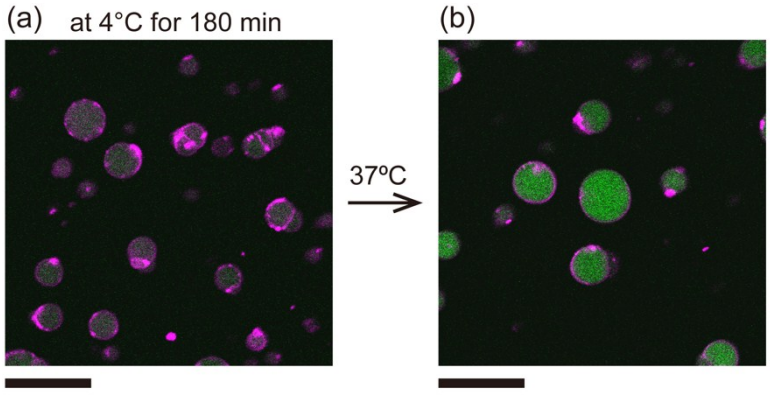

Fig. S4 Microscopic images of GUVs containing the amplification circuit with 10 nM signal incubated at (a) 4°C for 180 min and then at (b) 37°C for 20 min. The sample solution was deposited onto a glass slide with silicone rubber sheet and a coverslip. It was placed in a temperature-controlled room at 4°C. After incubation for 180 min, GUVs were visualised at 25°C, and then the sample was put on the heater at 37°C for 20 min and

visualised again.

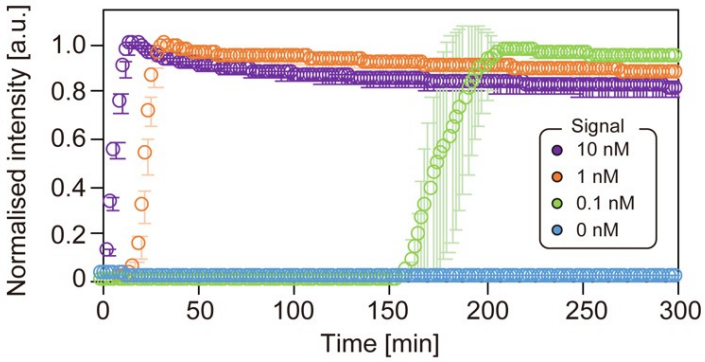

Fig. S5 Isothermal amplification reaction in test tubes, represented as the time series of change in green fluorescence intensity at signal concentrations of 10 nM (purple), 1 nM (orange), 0.1 nM (green), and 0 nM (light blue). Intensity of the samples with signals was normalised using maximum and minimum values measured during the observation in each plot. The value for 0-nM signal was normalised using maximum values of all samples and minimum values in the 0-nM signal sample; t = 0 indicates the time point when fluorescence intensity recording was started.

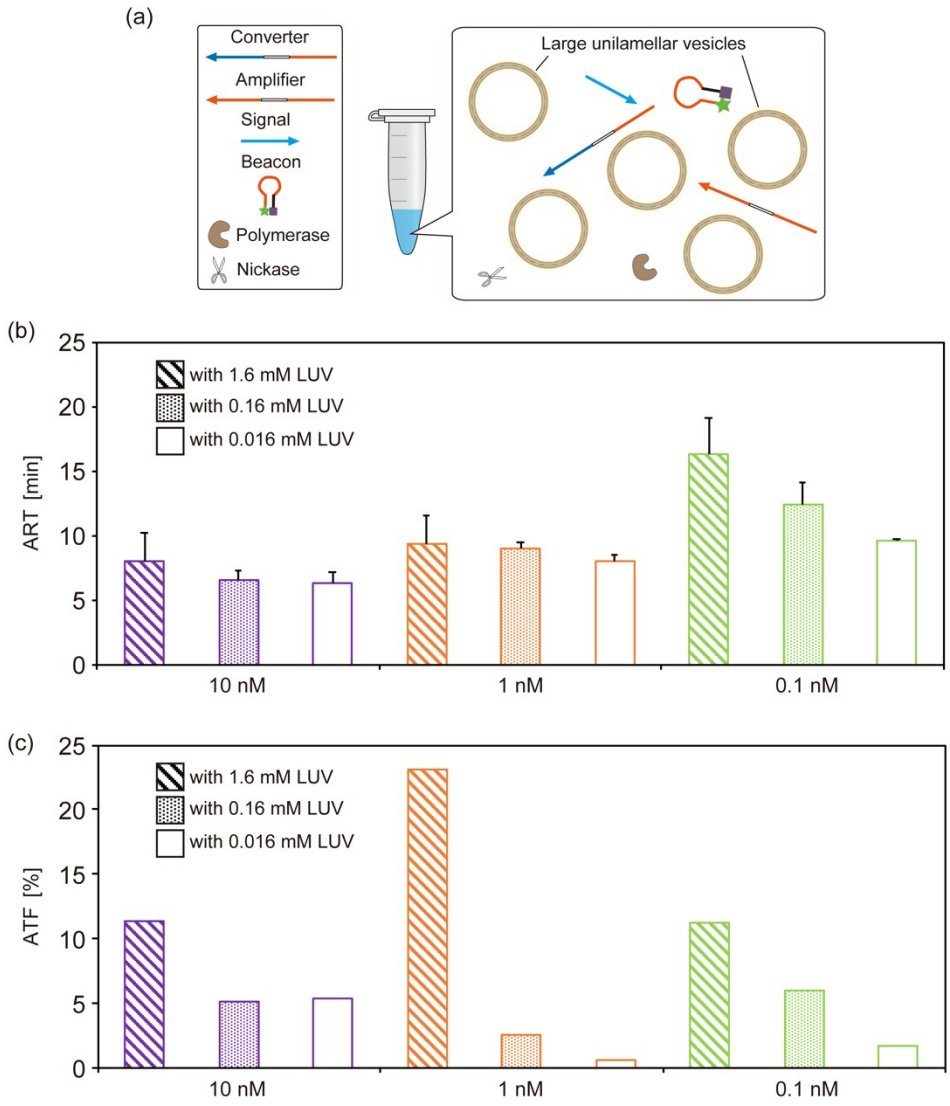

Fig. S6 Amplification characteristics in test tubes with large unilamellar vesicles (LUVs) at different total lipid concentrations. (a) Schematic representation of the experiment. The amplification circuit was mixed in a test tube with LUVs; (b) amplification rise time (ART); (c) amplification timing fluctuation (ATF).

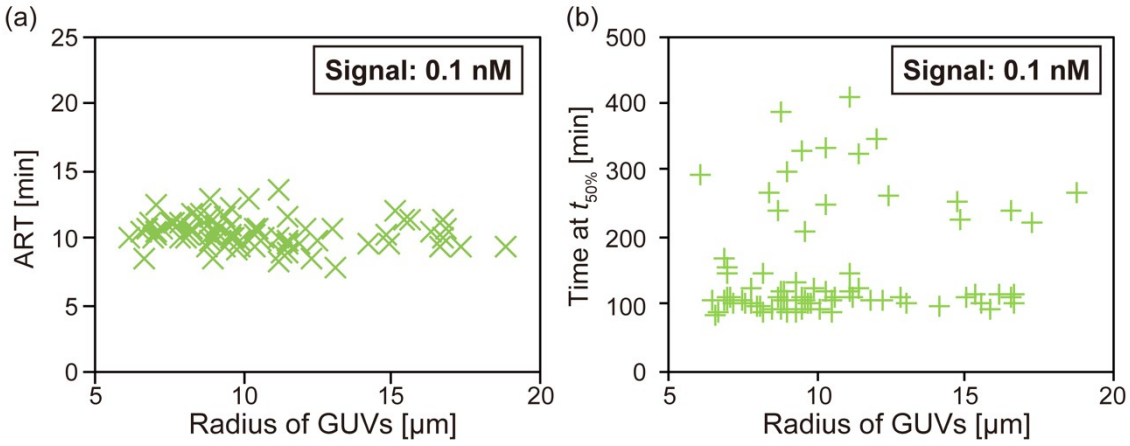

Fig. S7 (a) Effect of GUV size on the amplification rise time (ART) and (b) time at $t_{50\%}$ (50% value of the intensity compared to the maximum and minimum values) in 0.1 nM signal concentration. The radius of GUVs was measured from the area of cross-sectional images of GUVs visualised by confocal microscopy.

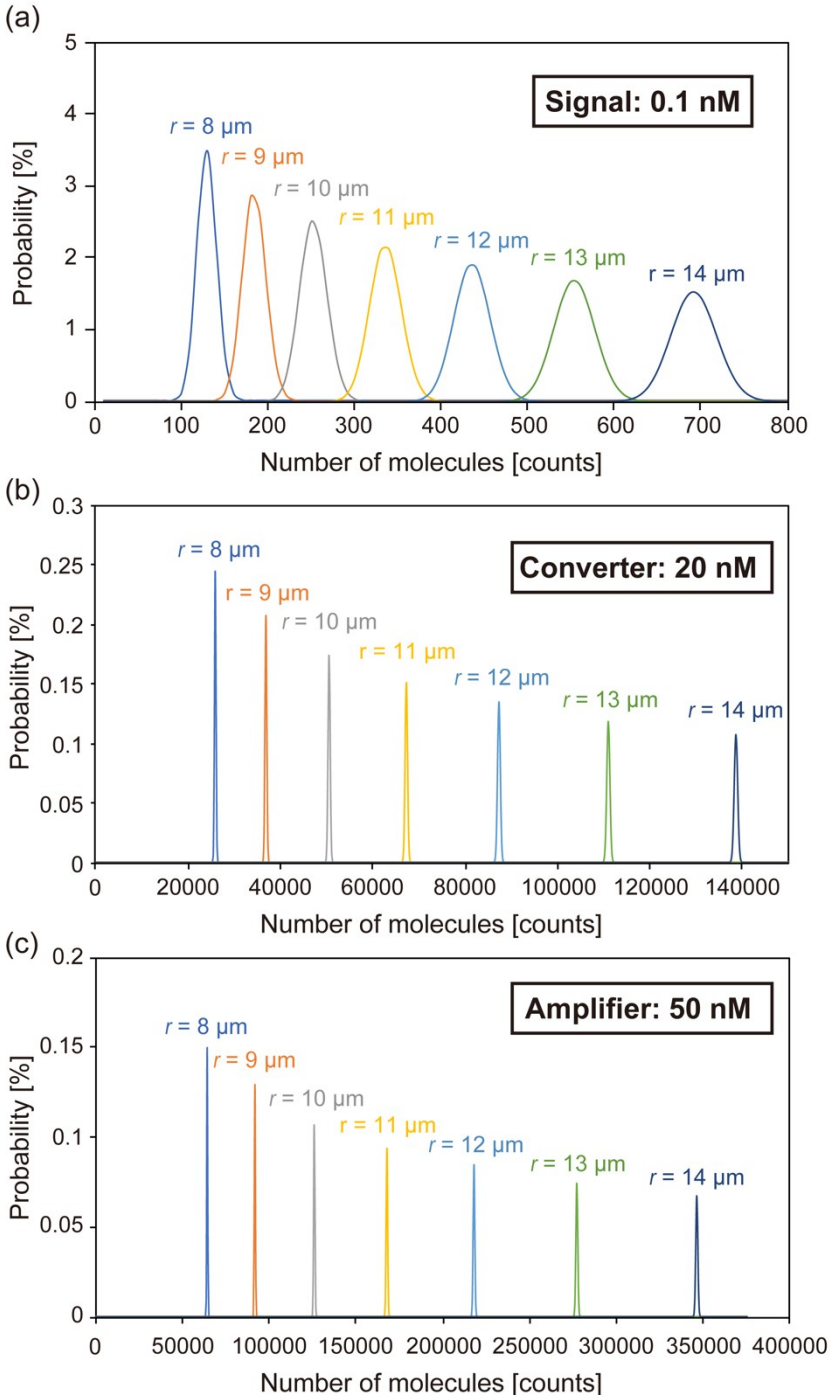

Fig. S8 Poisson distribution of the encapsulated DNAs across the average size-range of GUVs (8–14 µm radius): (a) 0.1 nM signal DNA; (b) 20 nM converter DNA; (c) 50 nM amplifier DNA.

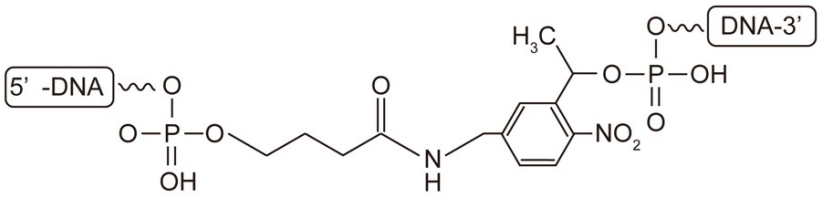

Fig. S9 Structural formula of a photo-cleavable site.

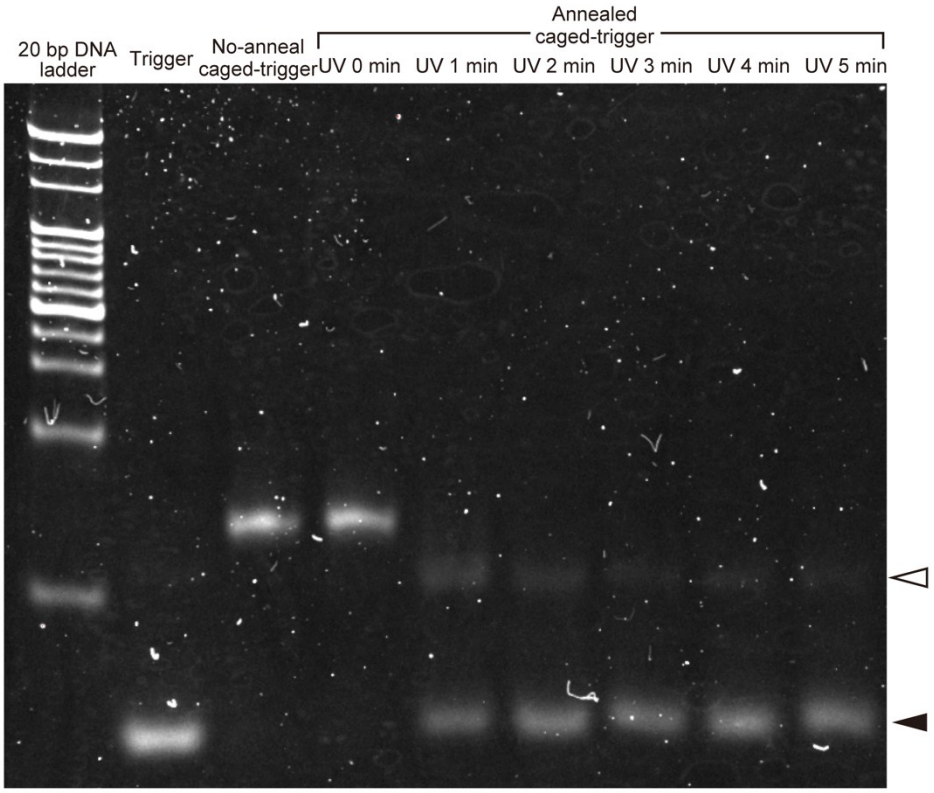

Fig. S10 Polyacrylamide gel electrophoresis to confirm the cutting efficiency of caged-signal at different UV irradiation times. After UV irradiation for 1 min, the band position shifted with respect to that of the unirradiated sample. In the lane for 1-min UV irradiation, a new band appeared at a position similar to that of the normal signal band (black triangle). This suggested that the photocleavable spacers were efficiently cut, and signal DNA generated by UV irradiation. A band of weak intensity had also appeared (open triangle), which disappeared in the lane for 5-min irradiation. Thus, we adopted 5-min UV-irradiation as the optimal condition.

References

1 (a) S. Pautot, B. J. Frisken and D. A. Weitz, *Langmuir*, 2003, **19**, 2870–2879; (b) S. Fujii, T. Matsuura, T. Sunami, T. Nishikawa, Y. Kazuta and T. Yomo, *Nat. Protoc.*, 2014, **9**, 1578–1591.

2 A.-N. Spiess, C. Feig and C. Ritz, *BMC Bioinformatics*, 2008, **9**, 221.

3 D. H. Mengistu, K. Bohinc and S. May, *J. Phys. Chem. B*, 2009, **113**, 12277–12282.

4 M. Weitz, J. Kim, K. Kapsner, E. Winfree, F. Franco and F. C. Simmel, *Nat. Chem.*, 2014, **6**, 295–302.

5 J. Olejnik, E. Krzymanska-Olejnik and K. J. Rothschild, *Nucleic Acids Res.*, 1996, **24**, 361–366.

6 S. Ueno, A. Ono, R. Kobayashi, Y. Tanaka, S. Sato, M. Biyani, N. Nemoto and T. Ichiki, *J. Photopolym. Sci. Technol.*, 2012, **25**, 67–72.

7. K. Komiya, M. Komori, C. Noda, S. Kobayashi, T. Yoshimura and M. Yamamura, *Org. Biomol. Chem.*, 2019, Advance Article, DOI: 10.1039/C9OB00521H.